

# Aerodynamics of Wraparound Fins

B. Bar-Haim\* and A. Seginer†

*Technion—Israel Institute of Technology, Haifa, Israel*

A possible reason for the induced rolling moments occurring on wraparound-fins (WAF) configurations in subsonic flight at zero angle of attack is suggested. The subsonic potential flow over the configuration at zero incidence is solved numerically. The body is simulated by a distribution of sources along its axis, and the fins are described by a vortex lattice method. It is shown that rolling moments can be induced on the antisymmetric fins by the radial flow generated at the base of the configuration, either over the converging separated wake or over the diverging plume of a rocket motor.

## Nomenclature

$C_l$	= rolling moment coefficient, normalized by body diameter and body cross-sectional area
$C_{l\delta}$	= rolling moment coefficient slope due to fins' deflection (1/deg)
$C_{lp}$	= roll damping moment coefficient (1/rad)
$C_p$	= pressure coefficient
$D$	= body diameter
$M$	= freestream Mach number
$P_j/P_\infty$	= rocket motor pressure ratio
$x, y, z$	= Cartesian coordinates system
$x_{sp}$	= wake length up to the rear stagnation point
$\delta$	= fin deflection angle, deg
$\theta_D$	= fin opening angle, deg
$\Lambda$	= fin edge sweep angle, deg
$\psi$	= fin span angle, deg

## Subscripts

$j$	= jet
LE	= leading edge
sp	= stagnation point
TE	= trailing edge
~	= freestream

## Introduction

THE last decade has seen the development of many tube-launched missiles, from ground-launched saturation field-artillery rockets to air-launched weapons, whether simple unguided rockets or sophisticated cruise missiles. Tube launching was chosen for its packaging convenience and for increasing the reliability of the rocket motor, but it also required folding aerodynamic stabilizers because of packaging constraints. Such stabilizers would be folded in the stowed position to fit within a circular cylinder and would deploy instantly after launch. Wraparound-fins (WAF) configurations (see, for example, Fig. 1) meet this requirement while they maximize the volume available for the missiles subsystems, especially for the nozzle exit.

It has been repeatedly observed that WAF configurations had conventional longitudinal aerodynamic characteristics (for example, Refs. 1-4) equal to those of configurations with planar fins of identical planform. However, as early as 1960, Featherstone<sup>1</sup> already pointed out that WAF configurations displayed a seemingly unpredictable lateral behavior. Of

special interest for the present investigation were the induced rolling moments. While these were understandable, if not predictable, at the higher angles of attack as a result of the asymmetry of the curved fins,<sup>4,5</sup> the rolling moments, measured at zero angle of attack,<sup>5</sup> and even more so the roll reversal when WAF configurations accelerated or decelerated through the sonic speed range,<sup>6</sup> presented an enigma. Due to the significance of WAF configurations in weapons technology and to their unusual lateral characteristics, an international research program, The Technical Cooperation Program<sup>7</sup> (TTCP) was set up at an international meeting at Eglin Air Force Base in 1969. In the ensuing research effort encompassing the U.S. Armed Forces, the United Kingdom, Canada, and Australia, an intensive experimental investigation program was launched to study the aerodynamic characteristics of a standard configuration (Fig. 1) with 20 different fins and two different bodies, at Mach numbers from 0.3 to 3.0.<sup>8-10</sup> The experimental results of this program proved that the static longitudinal aerodynamic characteristics of WAF configurations did not differ from those of conventional configurations with identical bodies and flat fins, whose area was equal to the projected area of the curved fins. This conclusion meant that WAF configurations could be used where flat fins had been used before, without any penalty in their longitudinal aerodynamics and even without a severe increase in their total drag. However, those results substantiated Featherstone's findings of unusual lateral aerodynamics. In spite of the relatively large scatter in the experimental data obtained from the sting-mounted models in the various wind tunnels involved,<sup>10</sup> there was no doubt that WAF configurations developed induced rolling moments, even at zero angle of attack. Generally speaking, these moments acted upon the fins in the direction of their center of curvature at subsonic speeds, and changed direction in transition to supersonic speeds or vice versa. This behavior could be detrimental to the stability of WAF missiles because roll resonance or pitch-roll lockin and catastrophic yaw due to roll-yaw coupling could develop at the point of roll reversal, increasing the scatter of such missiles around their targets.<sup>7</sup> Although the problem can be overcome by intentionally spinning the missile (by means of canted fins, for example), the TTCP participants still felt the need to identify the origin and understand the nature of the induced rolling moments. But, in spite of years of investigative effort, the answer eluded them.

Intrigued by this problem, the authors tried an analytic approach. A lifting-line theory for antisymmetric wings with spanwise curvature in uniform flow was developed, with the hope that the asymmetric tip vortices generated at any finite angle of attack may retain some vorticity when the angle is gradually decreased to zero. However, nothing but the trivial solution could be found at zero incidence. Next, the authors modified the vortex-lattice code for wings alone of Ref. 11 to

Received March 15, 1982; revision received Jan. 25, 1983. Copyright © American Institute of Aeronautics and Astronautics, Inc., 1982. All rights reserved.

\*Graduate Student, Dept. of Aeronautical Engineering.

†Associate Professor, Dept. of Aeronautical Engineering; currently National Research Council Research Associate, NASA Ames Research Center, Moffett Field, Calif. Member AIAA.

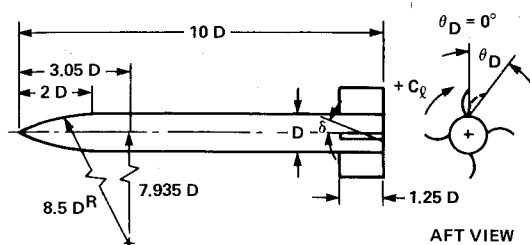


Fig. 1 Standard WAF configuration.<sup>7</sup>

handle antisymmetric, spanwise-curved wings. Again wraparound wings at zero incidence in uniform flow failed to produce rolling moments. With the failure of both of these approaches in uniform oncoming flow and with some experimental indication<sup>6</sup> that rocket motor burnout also gave rise to roll reversal, the authors suspected that, in subsonic flow, the rolling moments could be generated by a radial velocity component induced on the fins by the wake flowfield.

The purpose of this work was defined as an investigation of this idea and an effort to prove its feasibility. It was by *no means* meant to be a rigorous solution of the flowfield around a WAF configuration at any given angle of attack. Consequently, the authors decided to use existing approximate numerical methods with some simplifying assumptions in order to obtain at least a qualitative answer for minimum effort and cost.

### The Mathematical Model

The mathematical model, as well as the numerical methods used here, are well known and will be described only briefly. The interested reader should consult the relevant references for more details.

With no reason to anticipate any viscous effects in the mechanism generating the rolling moments, it is sufficient to describe the potential flow about the WAF configuration. If the flow is incompressible, this can be done by the well-known Laplace equation for the velocity potential with a tangency boundary condition on all the solid surfaces of the configuration. Further boundary conditions can be imposed, such as the Kutta condition at the fins' trailing edge and/or a prescribed wake geometry ("linear wake") or a force-free rolled-up wake ("nonlinear wake"). A problem described in this way can be solved in a given uniform flow by an assumed distribution of a discrete number of potential elemental functions (i.e., sources, doublets, and vortices) inside the body or on its surface. The intensities of these functions are determined by satisfying the boundary conditions, and with the intensities known, the induced-perturbation velocities at every point in the flowfield and the pressure distribution over the configuration's surfaces can be computed.

If the solution has to be extended into the subsonic compressible flow regime, as is done in this work, then the linearized, small-perturbation potential equation is transformed into the Laplace equation by the well-known Goethert transformation and the same solution procedure, described above, is used.

With this approach, what remains to be decided is the exact model of potential singular-elements distribution that is to be used in a certain case.

As stated previously, the purpose of this work was to identify, even if only qualitatively, a possible mechanism that could induce rolling moments on WAF configurations at zero angles of attack. It was therefore decided to use the simplest and least expensive numerical approach available. Consequently, the subsonic flowfield over WAF configurations was solved at zero angle of attack only. This restriction, while it did not severely limit the applicability of the calculated results since most WAF missiles fly at rather small angles of attack and the rolling moments at these angles are practically constant,<sup>8</sup> greatly simplified the modeling of the body and

saved computation time. It was assumed and later justified by the computed results that at zero angle of attack the solution could be uncoupled. Since the fins were not generating any lift, except for the minute amount necessary for the induced rolling moment, their effect on the flowfield and, consequently, on the solution for the body must be negligible. It was, therefore, decided to simulate first the body only by a distribution of sources along its axis, and then the fins in the presence of the body by a modification of the nonlinear vortex-lattice method of Ref. 11. This uncoupled solution served to minimize the computation time, especially as the body-induced flowfield had to be computed only once, and then could be used for all subsequent fin arrangements.

### Body Modeling

A good approximation of the body flowfield could have been obtained using one of the now classical source-panel methods (such as in Ref. 12). An even better approximation could have been obtained by the simultaneous solution for the complete interaction flowfield of the body and the wraparound surfaces with the method of Ref. 13. This method would have accounted also for the effects of the fins and their wakes on the body at finite angles of attack. However, such methods are time consuming and unjustified for a qualitative investigation such as this and, as later observed, not even necessary at zero angle of attack.

The actual description of the axisymmetric body at zero incidence in this work is by a distribution of a finite number of discrete point sources along its axis. The intensities of these sources are determined by satisfying the flow tangency boundary condition on the same number of control points on the body. The details of this well-established method are given by von Kármán<sup>14</sup> and not repeated here. Satisfaction of the boundary condition at one of the control points may be replaced by an imposed stagnation condition at the body apex in order to improve the accuracy of the solution in this region.<sup>15</sup> With the intensities of the sources known, the velocities induced by the body can be calculated at any point in the flowfield.

Obviously, the description of the body by a source distribution along its axis is valid for an axisymmetric body at zero incidence only. For any other case, a more sophisticated scheme (like that of Ref. 12) must be used; however, it sufficed for the needs of this investigation. Furthermore, the source distribution was computed only once in the absence of the fins (in order to save computation time) assuming that the fins' interaction on the body was negligible. This interaction was evaluated from the results of the complete program and the assumption was verified when it was found that the velocities induced by the fins on the body at zero incidence were negligible. This is to be expected because at this condition the fins do not generate lift and, therefore, do not disturb the flow.

### Wake Modeling

As mentioned before, when simulation of wraparound surfaces in uniform flow failed to produce rolling moments, the authors deduced from the roll-reversal at sonic speeds and from the opposite sense of the rolling moment when the WAF missile's rocket motor was firing that the wake structure must have an upstream influence (in subsonic flow) on the fins. A radial velocity component induced on the antisymmetric fins could generate an asymmetric load on the fins and, therefore, a rolling moment also.

With this in mind it became necessary to simulate not only the body but also its wake. Since the potential flow model used could not account for a wake (whether the viscous wake of the body or the plume of a rocket motor), the problem could be evaded by substituting a solid body for the inner wake enclosed by the dividing streamline. For this to be done the shape of the dividing streamline had to be known from external sources and the resulting "solid body" was in-

incorporated into the body simulation as if it were its inherent rear part.

Three types of wake shapes are simulated in this work: 1) the free undisturbed wake of a body in free flight; 2) the wake of a sting-mounted body in a wind tunnel; and 3) the plume of an underexpanded jet firing from a rocket motor exit nozzle. Wake shapes are not readily available in any single reference and a comprehensive literature review had to be undertaken in order to compile the necessary data.<sup>16</sup> In view of the length of the present paper as it stands, only the relevant conclusions of this review are given.

1) The diving streamline of a free wake was modeled by an ogival solid body. This shape was based on the experimental observations of Refs. 17-20. The flow visualization of Refs. 17-19 showed the separating streamline to leave the body tangential to the surface and to enter the rear stagnation point at an angle between 30 and 40 deg. The tangent-ogive offered a good simulation of this pattern (Fig. 2). The most important characteristic of the wake, namely its length to the rear stagnation point and its dependence on the Mach number (Fig. 2), was based on Ref. 18. No effect of the Reynolds number on the length and shape of the wake was found once the wake was turbulent.<sup>18,20</sup> The results of Ref. 20 with different base shapes indicated that the presence of the fins should have no effect on the shape and total length of the wake. When the computer code was finally run, the influence of variations in the wake shape were investigated. Various wake shapes (e.g., parabolic or cubic-polynomial) of equal length were tried, but the effects of these variations on the results were insignificant.<sup>16</sup>

2) Verification of the proposed mathematical model required a comparison with experimental data. However, such data were obtained from sting-mounted wind tunnel models. The sting changes the wake into that of a backward facing step, from an axisymmetric step<sup>19</sup> (large step height to body diameter ratio) to an almost two-dimensional step<sup>17</sup> (when the step is small). The location of the rear stagnation point (or reattachment point) on the sting has not been previously reported and the authors determined its approximate position from measured pressure distributions<sup>21</sup> and flow visualizations,<sup>19</sup> and defined an equivalent ogival afterbody by an extrapolated rear stagnation point on the axis (Fig. 2). The dependence of the length of this equivalent wake on the flow Mach number is shown in Fig. 2 for a body-to-sting diameter ratio of 3:1. This ratio was chosen because it is widely used by wind-tunnel operators and because it was used in the Arnold Engineering Development Center's (AEDC) 4-ft wind tunnel subsonic and transonic experiments reported by Dahlke.<sup>9</sup> Although the method of determining the position of the rear stagnation point is fairly crude, the influence of its

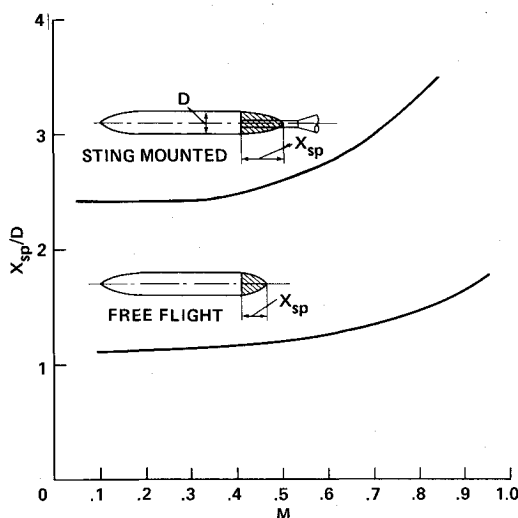


Fig. 2 Modeling of closed wake in free flight and on a sting mount.

inaccuracy was not large. The change in the induced rolling moment caused by a 20% variation in the length of the wake was in the range of 1-2%.

3) The third wake that was simulated was a rocket exhaust jet plume. WAF configurations are rocket powered and the induced rolling moments during the powered phase of the flight are also of interest.<sup>6</sup> The literature review of Ref. 16 defined a very large number of parameters that determined the shape of the plume. Since the prime target of this work was to obtain qualitative data on the induced rolling moments and since experimental data on these moments during powered flight were not available for comparison, the plume was modeled for a limited number of parameters only. These were for a sonic jet blowing from a cylindrical nozzle exit into a subsonic outer flow. The jets were underexpanded, with jet-to-freestream pressure ratios from 1 through 6. The typical geometrical features of the jet plume (the length of the first jet "diamond," its upstream vertex angle, and the diameter of its downstream end) under these conditions were taken from Refs. 22 and 23. With these three parameters specified, the shape of the solid body simulating the jet plume was modeled by a second-order polynomial.<sup>16</sup>

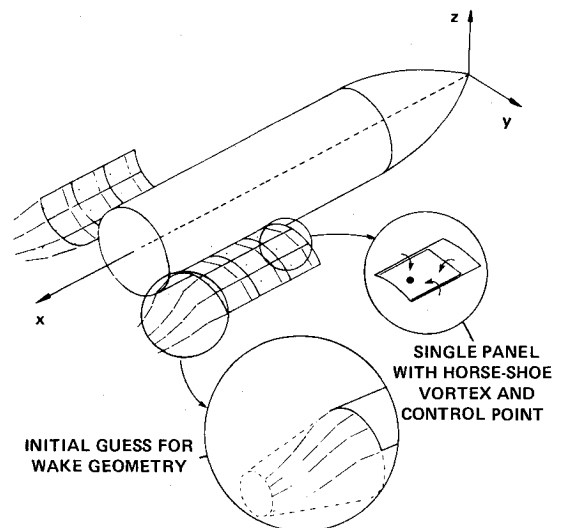


Fig. 3 Schematic modeling of WAF configurations.<sup>16</sup>

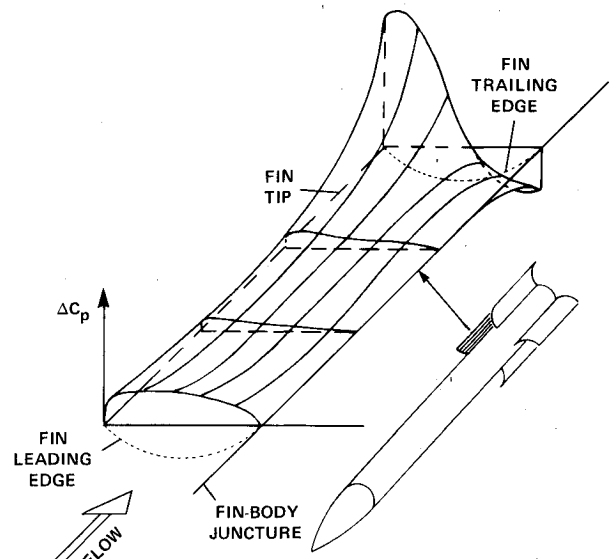


Fig. 4 Load distribution over fin on standard WAF configuration at  $M=0$  and zero angle of attack.

### Fin Modeling

With the body-induced flowfield known, the pressure loading on the fins can be calculated and integrated to produce the induced rolling moment. In the present work, this is done by a nonlinear vortex lattice method (VLM).<sup>11</sup> Each fin is divided into quadrilateral panels (Fig. 3), and bound-horseshoe vortices of unknown strength are distributed at the 1/4 chord positions of the panels (insert A in Fig. 3). The trailing vortices from the system are free to shed from the fins' trailing and side edges, and after determining their equilibrium position in space, they form the vortex wake of the fins. The intensities of the vortices are again determined by the tangency boundary condition. This condition is imposed at a finite number of control points located at the midspan of each panel's 3/4 chord line, and is satisfied by the mutual cancellation of the components that are normal to the fins' surfaces at the control points of the freestream velocity and body and vortex flowfields. The formulation of this tangency boundary condition at a given number of control points results in the same number of linear algebraic equations for the unknown intensities of the vortices. The solution of this system of equations requires, however, prior knowledge of the trajectories of the free vortices because the velocities induced by them on the control points have to be accounted for also. The trajectories, in themselves part of the solution, are either assumed to be known in the linear VLM codes or computed by an iterative process in the nonlinear VLM codes. In the latter case, an initial guess for the trajectories is needed. It is usually assumed that the free vortices trail off to infinity as straight lines. With the intensities of the vortices known, the free vortices are allowed to follow local streamlines. The vortex intensities are then recomputed and the process is reiterated until the vortex wake relaxes to its equilibrium rolled-up position. This nonlinear procedure was also followed in the present investigation.<sup>16</sup> However, it was found that since the fins were at zero incidence and the normal forces generated by them were of second order, their influence on the wake rollup was almost insignificant. Consequently, the contribution of the nonlinear process to the induced rolling moments was negligible and they could be computed by the linear version of the code (its first iteration only) at a considerable reduction (75%) in computation time.

With the strengths of the vortices known, the pressure distribution acting on the fins is computed by the Kutta-Joukowski theorem and is integrated relative to the body axis to give the rolling moment.

### Computational Results

The main purpose of this work, as stated earlier, is to identify a possible mechanism inducing rolling moments on WAF configurations at zero angle of attack. The preliminary study indicated that while no such moments could be produced in a uniform flowfield, the radial velocity component at the base of the configuration (inward over a closed wake or outward over a jetplume) could induce rolling moments by interacting with the antisymmetric fins.

To verify this hypothesis, even if only qualitatively, the computation results had to be compared with experimental data. No such data were available for WAF configurations in free flight so that wind-tunnel data generated by the TTCP<sup>7</sup> had to be used. This was the reason for the simulation of the wake of a sting-mounted model. There were, however, drawbacks to the use of these data. Not having been aware of the possibly decisive role of the wake flow in this case, the participants of the TTCP did not specify in their reports (e.g., Refs. 8-10) the model-to-sting diameter ratios. One cannot be certain even that the same ratio was used throughout the program. As shown in Fig. 2 this ratio has a first-order influence on the length of the wake and, consequently, should also have a non-negligible effect on the radial component of the velocity and on the rolling moments it induces. Since the

experiments reported in Ref. 9 were done with a body-to-sting diameter ratio of 3:1, which is the common practice in wind-tunnel work, and for lack of information to the contrary, it was assumed here that all the data were obtained with this ratio. This assumption may have contributed to the scatter in the data, which was considerable anyway because of the difficulties to measure accurately the relatively small rolling moment, especially at the lower subsonic Mach numbers.<sup>9</sup> The low accuracy of the experimental data limited the comparison with the computational results more to qualitative evaluation rather than full verification of the mathematical model.

### The Standard Model

The TTCP standard WAF configuration,<sup>9</sup> designated as B1F1 (Fig. 1) in the literature, was modeled for the comparison. The configuration was comprised of an axisymmetric body (a 2 diameter long ogive nose and an 8 caliber cylindrical body) and a cruciform of fully deployed wraparound fins of rectangular planform that completely encircle the body when folded (Figs. 1 and 3).

A distribution of a minimum of 50 sources was necessary for a reasonably smooth modeling of the body and its wake. The accuracy of the body modeling can be controlled by a comparison of the resulting body radius (of the zero streamline) between control points with the actual radius, and by comparison of the local computed flow direction at these points with the body slope. The number of the sources and their spacing along the axis are automatically adjusted until prescribed accuracy criteria are satisfied.

The modeling of the fins was done with 100 uniform vortex panels (Fig. 3) per fin. This fine division guaranteed the numerical accuracy of the results. For instance, an increase in the number of panels by 30% changed the computed rolling moment by less than 0.5%. The computed pressure distribution over a fin that is shown in Fig. 4 indicates that the number of panels could be decreased and computation time could be saved by a nonuniform spacing of the panels with a far lower density on the upstream three-quarters of the fin and a denser division on its aft quarter where the pressure gradients are large. Another method to save computation time at a penalty of a 2-3% error in the rolling moment was to model only one pair of fins on the configuration and multiply the computed moment by two. A linear solution for one pair of fins took about 125 s on an IBM 370/165 computer, while a cruciform fin configuration required about 500 s.

The linear solution needed a prescribed shape of the fins' vortex wake. Insert B in Fig. 3 describes the options for this shape. The first guess is that the free vortices lie on a truncated conical surface trailing the fin. The user can specify the length and vertex angle of this cone and even a spiral twist of the vortices over the cone as a simulation of the wake rollup. A nonlinear computation of the full wake rollup (found not to be necessary for the present purpose), would, of course, require considerably more computer time.

### Comparison with Experimental Data

The variation of the rolling moment coefficient for the standard WAF configuration with the Mach number is compared in Fig. 5 with the experimental data of Ref. 10. These data were obtained both with the fins in a cruciform (+) position and in a (x) position, and also with special miniature fin balances in addition to the main integral balance. The agreement between the computed results and the experimental data is good at Mach numbers 0.5 and 0.8. The discrepancy at  $M=0.3$  cannot be explained by the present model unless it is due to the low accuracy of the experimental data at low Mach numbers.<sup>9</sup> The general trend of the declining rolling moment with increasing Mach number is correctly obtained. The Goethert compressibility correction cannot be carried past  $M=0.8$  and the curve is extrapolated (dashed line) to the vanishing value measured at  $M=1.0$ .

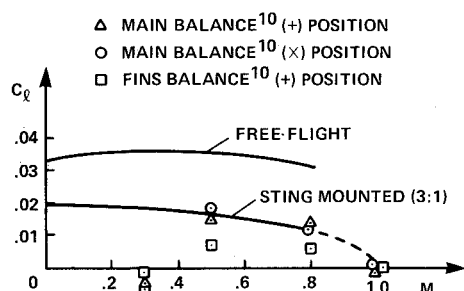


Fig. 5 Rolling moment coefficient compared with experimental data (standard WAF configuration).

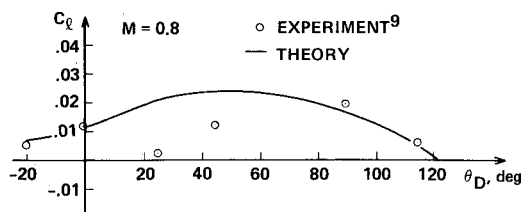


Fig. 6 Rolling moment coefficient vs fin opening angle compared with experimental data.

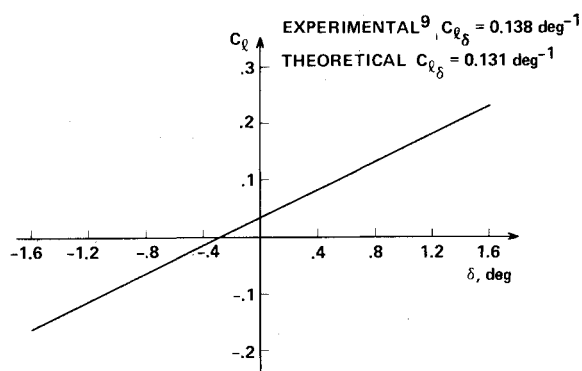


Fig. 7 Rolling moment coefficients due to fin differential deflection.

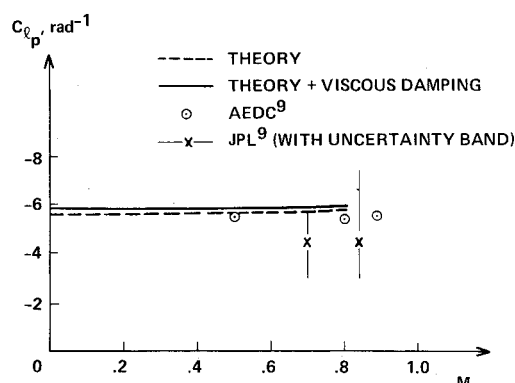


Fig. 8 Roll damping moment coefficient, including body contribution,<sup>16</sup> compared with experimental data.

Although not computable, this vanishing of the rolling moment at sonic speeds can be qualitatively explained by the present mathematical model. As the flow over the base of the body turns supersonic, the turning of the flow (either inward or outward in the wake region) is centered on the base corner, and cannot exert any influence upstream on the fins. Thus, the fins experience only parallel flow and, consequently, no rolling moment is developed. Comparisons with wind-tunnel results of other WAF configurations are given in Ref. 16 and

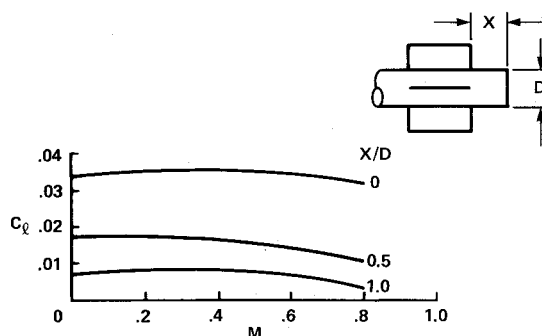


Fig. 9 Free flight rolling moment coefficient variation with fin axial position.

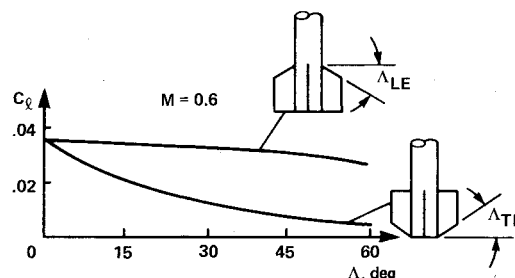


Fig. 10 Free flight rolling moment coefficient variation with leading-edge and trailing-edge sweep angle.

show the same kind of agreement as in Fig. 5. Also shown in Fig. 5 for comparison purposes is the rolling moment coefficient for the same configuration in free flight. The shorter and more rapidly closing wake in free flight almost doubles the computed rolling moments. These results could not be verified experimentally for lack of such data.

Other comparisons that were possible with experimental data are shown in Figs. 6-8. Figure 6 compares the rolling moment coefficients at  $M = 0.8$  for the standard configuration with the fins at different opening angles ( $\theta_D$ ), where at  $\theta_D = 120^\circ$  the fins are completely folded, and at  $\theta_D = 0^\circ$  they are fully deployed. Again, good agreement is observed, except for opening angles of 25 and 45 deg. No explanation can be offered for the discrepancy at these two angles. The same code was also used to compute the rolling moments generated by a small antisymmetrical deflection of the fins at an angle,  $\delta$ . Naturally the results are linear (Fig. 7). The computed slope of the curve,  $(C_{\ell})_{\delta} = 0.131/\text{deg}$ , falls close to the experimental value of  $(C_{\ell})_{\delta} = 0.138/\text{deg}$ . The final comparison was of the computed roll damping coefficient,  $C_{\ell p}$ , with experimental data. To compute this parameter the entire flowfield was spun around the configuration with a velocity distribution adopted from two concentric cylinders with the outer cylinder at infinity. The results are compared in Fig. 8 with data from the AEDC and Jet Propulsion Laboratory experiments reported in Ref. 9. The dashed line describes the results of the present mathematical model and the solid line is obtained from those by adding the roll damping due to the body boundary layer. The results are in fair agreement with the AEDC data (circles). Comparison with the JPL data is meaningless because of the large uncertainty levels reported for these data<sup>9</sup> (the AEDC data had no uncertainty levels shown<sup>9</sup>).

#### Parametric Study

Several other parameters were investigated, with details shown in Ref. 16. The following are some examples.

Since the main assumption here was that the base flow was responsible for the induced rolling moments, moving the fins upstream should weaken this moment. This effect is demonstrated in Fig. 9. Rolling moments for fins flush with the base plane are compared with those for fins moved up-

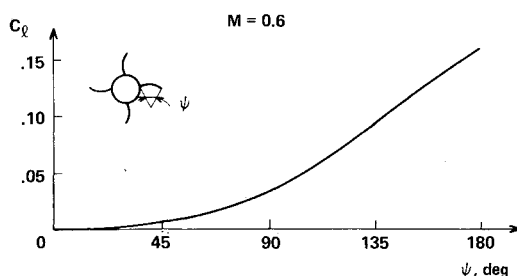


Fig. 11 Free flight rolling moment coefficient vs fin span angle.

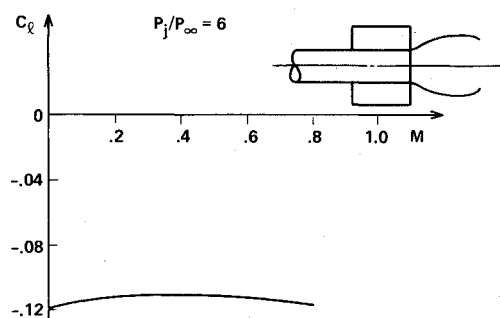


Fig. 12 Rolling moment coefficient with a 6:1 pressure ratio jet plume.

stream half a body diameter and one diameter, respectively. The rolling moment is clearly decreasing with increasing distance from the base and extrapolation seems to indicate that it might vanish at some upstream distance of 1.5 to 2.0 body diameters from the base. It is interesting to note in passing that the wraparound fins of Vought's MLRS missile are positioned upstream of the base.<sup>24</sup> However, no explanation was given for this design.

The strong effect of the proximity to the base is demonstrated also in Fig. 10, where the influence of fin leading-edge and trailing-edge sweep angle was studied. While leading-edge sweepback reduces the rolling moment only slightly, an identical forward sweep of the trailing edge sharply reduces the rolling moment. This result could be anticipated because most of the flow turning induced by the base flow would be felt by the aft portion of the fin, as was indeed demonstrated by the pressure distribution in Fig. 4. Moreover, most of the load there is carried by the outer aft-corner of the fin that is sliced off when the trailing edge is swept forward. While there is no experimental data available for swept-forward trailing edges, Ref. 9 reports results for swept-back leading edges. However the extremely large scatter in these data prevents any significant comparison. A possible experimental indication of the influence of the wake can be found in the strong effects that changes in the geometry of the fin trailing edge had on the rolling moment.<sup>25</sup>

The effect of the span of the fins is shown in Fig. 11. In certain missile designs the span of the fins is increased by increasing the sector angles ( $\Psi$ ) covered by the fins and by making them overlap (an arc angle of 90 deg is the common fin full span). As expected, the larger area of the fin generates a higher rolling moment, but the increase is not linear.

A further demonstration of the strong effect of the wake flow on the fins is presented in the rolling moments due to a jet plume of pressure ratio  $P_j/P_\infty = 6$  (Fig. 12). The results are shown for the only case of jet plume that was simulated (explained in the section on wake simulation) at the highest pressure ratio, because the rolling moment is then at its peak. For lower pressure ratios, the moment decreases in size and vanishes for an ideally expanded jet. As shown in Fig. 12 the outward radial component of the wake flow changes the direction of the rolling moment, which is now about four

times as great as the moment induced by the inward flow of the closed wake.

For additional examples (e.g., canard WAF, other asymmetric fin configurations, swept fins, etc.), the reader is referred to Ref. 16.

## Conclusions

By using a source-distribution simulation for the body and a vortex lattice simulation for the wraparound fins, it is shown that the radial velocity component induced on the fins by the wake flowfield could be responsible for the rolling moments encountered by WAF configurations in subsonic flow at zero angle of attack. No other mechanisms were found; however, their existence cannot be ruled out. The present simulation estimates rolling moments of the right magnitude and correct trends.

Assuming that the mechanism described by the present mathematical model is valid, the induced rolling moments could then be eliminated by mounting the fins about two body diameters upstream of the base of the body. Another method to prevent roll reversal in the accelerating phase is to accelerate into supersonic speed before the rocket motor burns out, because the roll direction in powered subsonic flight and in supersonic flight is the same.<sup>9</sup> This, however, will not solve the problem when the WAF configuration slows down to subsonic speeds at the end of its flight. The negative rolling moment experienced by WAF configurations in supersonic flow cannot be explained by the present purely subsonic mathematical model. It may be due to the shock wave focusing on the concave side of the curved fin with the resultant pressure difference acting in the direction of the convex surface. This hypothesis requires further theoretical work. More work will also be done on a parametric study of various effects on the rolling moments. It is also intended to apply the source-panel method<sup>13</sup> to describe the body and the nonlinear vortex lattice method for the fins in order to compute WAF aerodynamics at higher angles of attack.

## Acknowledgment

The work described herein was done in partial fulfillment of the requirements for the M.Sc. degree of B. Bar-Haim.

## References

- Featherstone, H.A., "The Aerodynamic Characteristics of Curved Tail Fin," Convair/Pomona Div., General Dynamics Corp., Pomona, Calif., GDC-ERR-PO-019, Sept. 1960.
- Stevens, F.L., On, T.J., and Clare, T.A., "Wrap-Around Vs. Cruciform Fins: Effects on Rocket Flight Performance," AIAA Paper 74-777, Aug. 1974.
- Lucero, E.F., "Subsonic Stability and Control Characteristics of Configurations Incorporating Wrap-Around Surfaces," *Journal of Spacecraft and Rockets*, Vol. 13, Dec. 1976, pp. 740-745.
- Sawyer, W., Monta, W., Carter, W., and Alexander, W., "Control Characteristics for Wrap-Around Fins on Cruise Missile Configurations," AIAA Paper 81-0009, Jan. 1981.
- Daniels, P. and Hardy, S.R., "Roll-Rate Stabilization of a Missile Configuration with Wrap-Around Fins," *Journal of Spacecraft and Rockets*, Vol. 13, July 1976, pp. 446-448.
- Mermagen, W.H. and Oskay, V., "Yaw-sonde Tests of 2.75-Inch Mk 66 Mod 1 Rocket," U.S. Army Armament Research and Development Command, Ballistic Research Lab., Aberdeen Proving Ground, Md., ARBRL-MR-03127, Aug. 1981.
- Holmes, J.E., "Wrap-Around Fin (WAF) Aerodynamics," *Proceedings of the 9th Navy Symposium on Aeroballistics*, Applied Physics Labs., The Johns Hopkins University, Md., Paper No. 4, May 1972.
- Dahlke, C.W. and Craft, J.C., "The Effect of Wrap-Around Fins on Aerodynamic Stability and Rolling Moment Variations," U.S. Army Missile Command, Redstone Arsenal, Ala., RD-TR-73-17, July 1973.
- Dahlke, C.W., "The Aerodynamic Characteristics of Wrap-Around Fins at Mach Numbers of 0.3 to 3.0," U.S. Army Missile Research, Development, and Engineering Lab., Redstone Arsenal, Ala., RD-77-4, Oct. 1976.

<sup>10</sup>Humphrey, J.A. and Dahlke, C.W., "A Summary of Aerodynamic Characteristics of Wrap-Around Fins from Mach 0.3 to 3.0," U.S. Army Missile Research and Development Command, Redstone Arsenal, Ala., TD-77-5, March 1977.

<sup>11</sup>Rom, J., Zorea, C., and Gordon, R., "On the Calculation of Nonlinear Aerodynamic Characteristics and the Near Vortex Wake," ICAS Paper No. 74-27, 1974.

<sup>12</sup>Woodward, F.A., "An Improved Method for the Aerodynamic Analysis of Wing-Body-Tail Configurations in Subsonic and Supersonic Flow," NASA CR-2228, May 1973.

<sup>13</sup>Rusak, Z., Wasserstrom, E., and Seginer, A., "Numerical Calculation of Nonlinear Aerodynamics of Wing-Body Configurations," *AIAA Journal*, July 1983, pp. 929-936.

<sup>14</sup>von Kármán, T., "Calculation of Pressure Distribution on Airship Hulls," NACA TM 574, 1930.

<sup>15</sup>Goodwin, F.K. and Dillenius, M.F.E., "Extension of the Method for Predicting Six-Degrees-of-Freedom Store Separation Trajectories at Speeds Up to the Critical Speed," USAF Flight Dynamics Lab., Wright-Patterson AFB, Ohio, AFFDL-TR-72-83, Oct. 1972.

<sup>16</sup>Bar-Haim, B., "Wrap-Around Fins Aerodynamics," M.Sc. Thesis, Technion—Israel Institute of Technology, June 1981.

<sup>17</sup>Rom, J., Victor, M., Reichenberg, M., and Salomon, M., "Wind Tunnel Measurements of the Base Pressure of an Axially Symmetric Model in Subsonic, Transonic and Supersonic Speeds at High

Reynolds Numbers," Technion—Israel Institute of Technology, Haifa, Israel, TAE Rept. 134, July 1972.

<sup>18</sup>Merz, R.A., "Subsonic Axisymmetric Near Wake Studies," *AIAA Journal*, Vol. 16, July 1978, pp. 656-659.

<sup>19</sup>Little, B.H. and Whipkey, R.R., "Locked Vortex Afterbodies," *Journal of Aircraft*, Vol. 16, May 1979, pp. 296-302.

<sup>20</sup>Gai, S.L. and Patil, S.R., "Subsonic Axisymmetric Base Flow Experiments with Base Modifications," *Journal of Spacecraft and Rockets*, Vol. 17, Jan.-Feb. 1980, pp. 42-46.

<sup>21</sup>Weeks, T.M. and Allen, N., "Base Flow Studies in/and Calibration of the New 15-Inch AFFDL Transonic Facility," USAF Flight Dynamics Lab., Wright-Patterson AFB, Ohio, unpublished data, May 1972.

<sup>22</sup>Lee, G., "An Investigation of the Transonic Flow Fields Surrounding Hot and Cold Sonic Jets," NASA TN D-853, April 1961.

<sup>23</sup>Love, E.S., Grigsby, C.E., Lee, L.P., and Woolding, M.J., "Experimental and Theoretical Studies of Axisymmetric Free Jets," NASA TR R-6, 1959.

<sup>24</sup>"Army MLRS Test-Launched at White Sands," *Aviation Week and Space Technology*, Vol. 112, June 9, 1980, p. 52.

<sup>25</sup>Bergbauer, D.M., Bergman, R.W., and Bentley, R., "Spin Profile Tailoring for the Improved 2.75" Rocket," AIAA Paper 80-1575, 1980.

## *From the AIAA Progress in Astronautics and Aeronautics Series*

# SPACECRAFT RADIATIVE TRANSFER AND TEMPERATURE CONTROL—v. 83

*Edited by T.E. Horton, The University of Mississippi*

Thermophysics denotes a blend of the classical engineering sciences of heat transfer, fluid mechanics, materials, and electromagnetic theory with the microphysical sciences of solid state, physical optics, and atomic and molecular dynamics. This volume is devoted to the science and technology of spacecraft thermal control, and as such it is dominated by the topic of radiative transfer. The thermal performance of a system in space depends upon the radiative interaction between external surfaces and the external environment (space, exhaust plumes, the sun) and upon the management of energy exchange between components within the spacecraft environment. An interesting future complexity in such an exchange is represented by the recent development of the Space Shuttle and its planned use in constructing large structures (extended platforms) in space. Unlike today's enclosed-type spacecraft, these large structures will consist of open-type lattice networks involving large numbers of thermally interacting elements. These new systems will present the thermophysicist with new problems in terms of materials, their thermophysical properties, their radiative surface characteristics, questions of gradual radiative surface changes, etc. However, the greatest challenge may well lie in the area of information processing. The design and optimization of such complex systems will call not only for basic knowledge in thermophysics, but also for the effective and innovative use of computers. The papers in this volume are devoted to the topics that underlie such present and future systems.

552 pp., 6 × 9, illus., \$30.00 Mem., \$45.00 List

TO ORDER WRITE: Publications Dept., AIAA, 1290 Avenue of the Americas, New York, N. Y. 10019